Analysis of Diffraction of Dominant Mode in an Acoustic Impedance Loaded Trifurcated Duct

Muhammad Ayub, Mazhar Hussain Tiwana, and Amer Bilad Mann

Department of Mathematics, Quaid-i-Azam University, Islamabad 44000, Pakistan

Reprint requests to M. H. T.; E-mail: mayub59@yahoo.com

Z. Naturforsch. **65a,** 995 – 1008 (2010); received September 15, 2009 / revised January 13, 2010

The paper presents the analytical description of diffraction phenomena of sound at the opening of a two dimensional semi-infinite acoustically soft duct. This soft duct is symmetrically located inside an infinite duct with normal impedance boundary conditions in the case where the surface acoustic impedances of the upper and lower infinite plates are different from each other. A matrix Wiener-Hopf equation associated with a new canonical scattering problem is solved explicitly. A new kernel function arose for the problem and has been factorized. The graphical results are also presented which show how effectively the unwanted noise can be reduced by proper selection of different parameters.

Key words: Sound Diffraction; Lined Duct; Integral Transform; Wiener-Hopf Technique; Expansion Coefficients; Pole Removal Technique.

1. Introduction

The waveguide elements are frequently used in many technical and industrial devices where they become a source of harmful and undesired noise. The phenomena occurring at the duct outlet is an important area in noise reduction and relevant for many applications. Continued interest in the problem of noise reduction has attracted the attention of many scientists, physicists, and numerical simulists. The studies of diffraction for different geometric designs with different combinations of the boundary conditions (soft, hard, impedance) are the topics of current interest in waveguides [1 – 8]. Historically the story goes that Jones [9] calculated the far field and the field within the waveguide by discussing the scattering of a plane wave from three parallel soft semi-infinite and equidistant plates. Asghar et al. [10] extended Jones' analysis [9] for the case of line source and point source scattering in still air and convective medium. Asghar and Hayat [11] studied the scattering of a plane acoustic wave by considering absorbtion at semi-infinite parallel plates. Rawlins and Hassan [12] analyzed the problem of acoustic radiation by taking into account a dominant surface wave mode in a semi-infinite waveguide. Note that the semi-infinite waveguide which supports surface waves is placed symmetrically in an acoustically lined infinite waveguide. They performed the Wiener-Hopf analysis for the trailing edge situation. Ayub et al. [13] studied the sound radiation by considering a trifurcated waveguide. The boundary conditions used in the mathematical problem are soft/hard for semi-infinite planes and acoustically impedance (with different impedances) for infinite planes. The analysis of the problem leads to two coupled Wiener-Hopf equations which were uncoupled by using the pole removal technique. This technique was introduced by Abrahams [14] and is now extensively available in the literature [15 – 18].

Keeping in view the above configurations, we analyzed the problem for the semi-infinite soft duct placed symmetrically inside an infinite acoustically lined duct. The surface impedances of the upper and lower infinite plates are different from each other. Using the Fourier transform, we obtain two simultaneous Wiener-Hopf equations. These equations are uncoupled by using the Wiener-Hopf procedure and the pole removal technique. The unknown constants involved in two infinite system of algebraic equations are evaluated numerically by using the approach employed by Rawlins [19]. The scattering of waves at the open end of the inner duct is determined. The physical model of the present problem is sketched in Figure 1.

The present paper is organized as follows: In Section 2 the problem statement is shown. The Wiener-Hopf (WH) equations have been formulated in Section 3 and the solution of the problem further devel-

0932–0784 / 10 / 1100–0995 $ 06.00

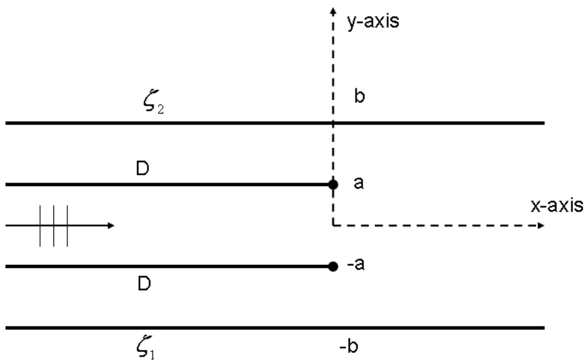

Fig. 1. Schematic diagram of two-dimentional channel.

oped in Section 4 whereas Section 5 is related to the reflected field representation. In Section 6 the graphs are displayed and discussed. Consequently, Section 7 consists of final remarks. The explicit factorization of the kernel functions has been accomplished in the appendix.

2. Problem Statement

The diffraction of the first mode of the inside waveguide (which is the only propagative mode) as incident mode that propagates out of the end of a semi-infinite soft duct is considered in this analysis. The wave mode is propagating in the positive x-direction parallel to the x-axis. The semi-infinite soft duct is placed inside the absorbingly lined duct with different acoustic impedances. If $\phi(x,y,t)$ is an acoustic scalar potential, then the acoustic velocity $\mathbf{u}$ and acoustic pressure p can be written as

$$\mathbf{u} = \operatorname{grad}\phi, \quad p = -\rho_0 \frac{\partial \phi}{\partial t},$$

respectively, where grad is the gradient operator, ρ_0 the density, and t the time. Writing

$$\phi(x,y,t) = \operatorname{Re}\{\mathrm{e}^{-\mathrm{i}\omega t}\Phi(x,y)\},$$

and omitting $\mathrm{e}^{-\mathrm{i}\omega t}$ throughout, we have to solve the following Helmholtz equation:

$$\frac{\partial^2 \Phi}{\partial x^2} + \frac{\partial^2 \Phi}{\partial y^2} + k^2 \Phi = 0, \tag{1}$$

where $k = \omega/c$ (ω is the angular frequency and c is the speed of sound) is the wave number. The wave number $k = k_1 + \mathrm{i}k_2$ has a small positive imaginary part which has been introduced to ensure the convergence (regularity) of the Fourier transform integrals defined subsequently in (16). The boundary conditions and continuity conditions associated with the problem are of the form:

$$\Phi + \left(\frac{\mathrm{i}\zeta_2}{k}\right)\frac{\partial \Phi}{\partial y} = 0, \quad y = b, \quad -\infty < x < \infty, \tag{2}$$

$$\Phi = 0, \quad y = a, \quad -\infty < x < 0, \tag{3}$$

$$\Phi = 0, \quad y = -a, \quad -\infty < x < 0, \tag{4}$$

$$\Phi - \left(\frac{\mathrm{i}\zeta_1}{k}\right)\frac{\partial \Phi}{\partial y} = 0, \quad y = -b, \quad -\infty < x < \infty, \tag{5}$$

$$\frac{\partial \Phi(x,-a^+)}{\partial y} = \frac{\partial \Phi(x,-a^-)}{\partial y}, \quad x > 0, \tag{6}$$

and

$$\frac{\partial \Phi(x,a^+)}{\partial y} = \frac{\partial \Phi(x,a^-)}{\partial y}, \quad x > 0, \tag{7}$$

where it is assumed that $b > a$. The associated boundary conditions given in (3) and (4) are acoustically termed as Dirichlet (soft) boundary conditions and correspond to the surfaces having infinite complex admittance [5]. The boundary conditions given in (2) and (5) represent general third-type impedance boundary conditions of the Robin type [3]. (6) and (7) show the continuity behaviour of the field across $y = a$ and $y = -a$ ($x > 0$), respectively [3]. In (2) and (5), $\zeta_{1,2}$ represent the specific impedances of the infinite duct lining, and it is necessary that for an absorbent surface $\operatorname{Re}\zeta_{1,2} > 0$ [20].

Besides the conditions prescribed in (2) – (7), we require those conditions at infinity which are relevant to the nature of the lowest propagating modes in various duct regions. The radiation conditions at infinity suggest the following [5]:

i) For the region $(-a \le y \le a, x < 0)$, one may write

$$\Phi(x,y) = \mathrm{e}^{\mathrm{i}\chi_1 x}\sin\left[\frac{\pi(y-a)}{2a}\right] + \sum_{n=1}^{\infty} R_n \mathrm{e}^{-\mathrm{i}\chi_n x}\sin\left[\frac{n\pi(y-a)}{2a}\right], \tag{8}$$

where $\chi_n = (k^2 - \alpha_n^2)^{\frac{1}{2}}$, $(n = 1,2,3,\ldots)$, and α_n satisfies

$$\sin 2(\alpha_n a) = 0, \tag{9}$$

where $\alpha_n = n\pi/2a$ with $0 < \mathrm{Im}\,\chi_1 < \mathrm{Im}\,\chi_2 < \mathrm{Im}\,\chi_3 \ldots$. The lowest-order plane wave mode can propagate only when $\pi/2 < ka < \pi$.

ii) The value of $\Phi(x,y)$ for $(-b \le y \le b,\, x > 0)$ is

$$\Phi(x,y) = \sum_{n=1}^{\infty} T_n \mathrm{e}^{\mathrm{i}\sigma_n x}\left[-\sin\beta_n(y-b) + \frac{\mathrm{i}\zeta_2}{k}\beta_n \cos\beta_n(y-b)\right], \tag{10}$$

where $\sigma_n = (k^2-\beta_n^2)^{\frac{1}{2}}$ $(n = 1,2,3,\ldots)$, and β_n satisfies the equation

$$\sin 2(b\beta_n) + \mathrm{i}\beta_n \frac{\zeta_1}{k}\cos 2(b\beta_n) + \mathrm{i}\beta_n \frac{\zeta_2}{k}\cos 2(b\beta_n) + \beta_n^2 \frac{\zeta_1\zeta_2}{k^2}\sin 2(b\beta_n) = 0, \tag{11}$$

with $0 < \mathrm{Im}\,\sigma_1 < \mathrm{Im}\,\sigma_2 < \mathrm{Im}\,\sigma_3 \ldots$.

iii) For $(a \le y \le b, x < 0)$ one has

$$\Phi(x,y) = \sum_{n=1}^{\infty} \widetilde{T}_n \mathrm{e}^{-\mathrm{i}\widetilde{\alpha}_n x}\left[-\sin\widetilde{\nu}_n(y-b) + \frac{\mathrm{i}\zeta_2}{k}\widetilde{\nu}_n \cos\widetilde{\nu}_n(y-b)\right], \tag{12}$$

where $\widetilde{\alpha}_n = (k^2-\widetilde{\nu}_n^2)^{\frac{1}{2}}$ $(n = 1,2,3\ldots)$, and $\widetilde{\nu}_n$ represent the roots of the equation

$$\sin\widetilde{\nu}_n(b-a) + \frac{\mathrm{i}\zeta_2}{k}\widetilde{\nu}_n \cos\widetilde{\nu}_n(b-a) = 0. \tag{13}$$

iv) When $(-b \le y \le -a,\, x < 0)$, we have

$$\Phi(x,y) = \sum_{n=1}^{\infty} \widehat{T}_n \mathrm{e}^{-\mathrm{i}\widehat{\alpha}_n x}\left[\sin\widehat{\nu}_n(y+b) + \frac{\mathrm{i}\zeta_1}{k}\widehat{\nu}_n \cos\widehat{\nu}_n(y+b)\right], \tag{14}$$

where $\widehat{\alpha}_n = (k^2-\widehat{\nu}_n^2)^{\frac{1}{2}}$ $(n = 1,2,3\ldots)$, and $\widehat{\nu}_n$ are the roots of the equation

$$\sin\widehat{\nu}_n(b-a) + \frac{\mathrm{i}\zeta_1}{k}\widehat{\nu}_n \cos\widehat{\nu}_n(b-a) = 0.$$

In the region $(-a \le y \le a,\, x < 0)$ the acoustic wave exhibits incident and reflected behaviour, while in the regions $(-b \le y \le -a,\, x < 0)$ and $(a \le y \le b,\, x < 0)$ transmission behaviour is observed. In the text R_n and T_n represent reflection and transmission coefficients, respectively.

To arrive at a unique solution we also require the 'edge conditions' [21]

$$\Phi(x,\pm a) = O(1) \;\text{ and }\; \Phi_y(x,\pm a) = O(x^{-\frac{1}{2}}) \quad \text{as } x \to 0. \tag{15}$$

3. The Wiener-Hopf (WH) Equations

For analytic convenience, we shall assume that $k = k_1 + \mathrm{i}k_2$ $(k_1 > 0, k_2 \ge 0)$ since the time dependence is taken to be of the form $\mathrm{e}^{-\mathrm{i}\omega t}$ [22]. Let us define the Fourier transform and its inverse by

$$\widehat{\Phi}(\alpha,y) = \int_{-\infty}^{\infty} \Phi(x,y)\mathrm{e}^{\mathrm{i}\alpha x}\mathrm{d}x = \widehat{\Phi}_+(\alpha,y) + \widehat{\Phi}_-(\alpha,y) \tag{16}$$

and

$$\Phi(x,y) = \frac{1}{2\pi}\int_{-\infty}^{\infty} \widehat{\Phi}(\alpha,y)\mathrm{e}^{-\mathrm{i}\alpha x}\mathrm{d}\alpha. \tag{17}$$

In (16)

$$\widehat{\Phi}_+(\alpha,y) = \int_0^{\infty} \Phi(x,y)\mathrm{e}^{\mathrm{i}\alpha x}\mathrm{d}x \tag{18}$$

and

$$\widehat{\Phi}_-(\alpha,y) = \int_{-\infty}^{0} \Phi(x,y)\mathrm{e}^{\mathrm{i}\alpha x}\mathrm{d}x, \tag{19}$$

where α is a complex variable as

$$\alpha = \mathrm{Re}\,\alpha + \mathrm{Im}\,\alpha = \sigma + \mathrm{i}\tau.$$

Use of (16) to (1) gives

$$\frac{\mathrm{d}^2\widehat{\Phi}}{\mathrm{d}y^2} + \kappa^2\widehat{\Phi} = 0, \tag{20}$$

where

$$\kappa(\alpha) = \sqrt{k^2-\alpha^2}. \tag{21}$$

The suitable solutions of (20) in the trifurcated regions are

$$\widehat{\Phi}(\alpha,y) = A_1(\alpha)\cos\kappa y + B_1(\alpha)\sin\kappa y, \quad -b \le y \le -a, \tag{22}$$

$$\widehat{\Phi}(\alpha,y) = \frac{-\mathrm{i}}{\chi_1+\alpha}\sin\left[\frac{\pi(y-a)}{2a}\right] + (A_2(\alpha)\cos\kappa y + B_2(\alpha)\sin\kappa y), \quad -a \le y \le a, \tag{23}$$

$$\widehat{\Phi}(\alpha,y) = A_3(\alpha)\cos\kappa y + B_3(\alpha)\sin\kappa y, \quad a \le y \le b. \tag{24}$$

By taking the Fourier transform, (2) to (7) become

$$\widehat{\Phi}(\alpha,b)+\left(\frac{\mathrm{i}\zeta_2}{k}\right)\widehat{\Phi}'(\alpha,b)=0, \tag{25}$$

$$\widehat{\Phi}_-(\alpha,a)=0, \tag{26}$$

$$\widehat{\Phi}_-(\alpha,-a)=0, \tag{27}$$

$$\widehat{\Phi}(\alpha,-b)-\left(\frac{\mathrm{i}\zeta_1}{k}\right)\widehat{\Phi}'(\alpha,-b)=0, \tag{28}$$

$$\widehat{\Phi}'_+(\alpha,-a^+)=\widehat{\Phi}'_+(\alpha,-a^-), \tag{29}$$

$$\widehat{\Phi}'_+(\alpha,a^+)=\widehat{\Phi}'_+(\alpha,a^-), \tag{30}$$

where the prime denotes the differentiation with respect to y. In order to determine $A_j(\alpha)$ and $B_j(\alpha)$ $(j=1-3)$, which are as yet unknown, we proceed to satisfy the boundary conditions (25) to (28). Thus, by invoking (27) and (28) in (22) we may write

$$A_1(\alpha)\cos\kappa a-B_1(\alpha)\sin\kappa a=\Phi_1^+(\alpha), \tag{31}$$

$$\begin{aligned}&A_1(\alpha)\left(\cos\kappa b-\left(\frac{\mathrm{i}\zeta_1}{k}\right)\kappa\sin\kappa b\right)\\&-B_1(\alpha)\left(\sin\kappa b+\left(\frac{\mathrm{i}\zeta_1}{k}\right)\kappa\cos\kappa b\right)=0,\end{aligned} \tag{32}$$

where $\Phi_1^+(\alpha)=\widehat{\Phi}_+(\alpha,-a)$ is analytic in $\operatorname{Im}\alpha>-\operatorname{Im}k$. Solving the above equations for $A_1(\alpha)$ and $B_1(\alpha)$ we obtain

$$A_1(\alpha)=\frac{\sin\kappa b+(\frac{\mathrm{i}\zeta_1}{k})\kappa\cos\kappa b}{\sin\kappa(b-a)+(\frac{\mathrm{i}\zeta_1}{k})\kappa\cos\kappa(b-a)}\Phi_1^+(\alpha), \tag{33}$$

$$B_1(\alpha)=\frac{\cos\kappa b-(\frac{\mathrm{i}\zeta_1}{k})\kappa\sin\kappa b}{\sin\kappa(b-a)+(\frac{\mathrm{i}\zeta_1}{k})\kappa\cos\kappa(b-a)}\Phi_1^+(\alpha). \tag{34}$$

Again, using (26) and (27) in (23), we may write

$$A_2(\alpha)\cos\kappa a+B_2(\alpha)\sin\kappa a=\Phi_2^+(\alpha), \tag{35}$$

$$A_2(\alpha)\cos\kappa a-B_2(\alpha)\sin\kappa a=\Phi_1^+(\alpha), \tag{36}$$

where $\Phi_2^+(\alpha)=\widehat{\Phi}_+(\alpha,a)$ is analytic in $\operatorname{Im}\alpha>-\operatorname{Im}k$. Solving (35) and (36) for $A_2(\alpha)$ and $B_2(\alpha)$, we obtain

$$A_2(\alpha)=\frac{\sin\kappa a(\Phi_1^+(\alpha)+\Phi_2^+(\alpha))}{\sin 2\kappa a}, \tag{37}$$

$$B_2(\alpha)=\frac{\cos\kappa a(\Phi_2^+(\alpha)-\Phi_1^+(\alpha))}{\sin 2\kappa a}. \tag{38}$$

With the use of (25) and (26) in (24), we may write

$$\begin{aligned}&A_3(\alpha)\left(\cos\kappa b-\left(\frac{\mathrm{i}\zeta_2}{k}\right)\kappa\sin\kappa b\right)\\&+B_3(\alpha)\left(\sin\kappa b+\left(\frac{\mathrm{i}\zeta_2}{k}\right)\kappa\cos\kappa b\right)=0,\end{aligned} \tag{39}$$

$$A_3(\alpha)\cos\kappa a+B_3(\alpha)\sin\kappa a=\Phi_2^+(\alpha). \tag{40}$$

Solving for $A_3(\alpha)$ and $B_3(\alpha)$, we obtain

$$A_3(\alpha)=\frac{\sin\kappa b+(\frac{\mathrm{i}\zeta_2}{k})\kappa\cos\kappa b}{\sin\kappa(b-a)+(\frac{\mathrm{i}\zeta_2}{k})\kappa\cos\kappa(b-a)}\Phi_2^+(\alpha), \tag{41}$$

$$B_3(\alpha)=-\frac{\cos\kappa b-(\frac{\mathrm{i}\zeta_2}{k})\kappa\sin\kappa b}{\sin\kappa(b-a)+(\frac{\mathrm{i}\zeta_2}{k})\kappa\cos\kappa(b-a)}\Phi_2^+(\alpha). \tag{42}$$

By substituting the above values of $A_j(\alpha)$ and $B_j(\alpha)$ $(j=1-3)$ in (22) to (24), we get

$$\begin{aligned}&\widehat{\Phi}(\alpha,y)=\\&\frac{\sin\kappa(y+b)+(\frac{\mathrm{i}\zeta_1}{k})\kappa\cos\kappa(y+b)}{\sin\kappa(b-a)+(\frac{\mathrm{i}\zeta_1}{k})\kappa\cos\kappa(b-a)}\Phi_1^+(\alpha),\\&-b\le y\le -a.\end{aligned} \tag{43}$$

$$\begin{aligned}\widehat{\Phi}(\alpha,y)&=\frac{-\mathrm{i}}{\chi_1+\alpha}\sin\left[\frac{\pi(y-a)}{2a}\right]+\frac{1}{\sin 2\kappa a}\\&\cdot(\Phi_2^+(\alpha)\sin\kappa(y+a)-\Phi_1^+(\alpha)\sin\kappa(y-a)),\\&-a\le y\le a,\end{aligned} \tag{44}$$

$$\begin{aligned}&\widehat{\Phi}(\alpha,y)=\\&\frac{\sin\kappa(b-y)+(\frac{\mathrm{i}\zeta_2}{k})\kappa\cos\kappa(y-b)}{\sin\kappa(b-a)+(\frac{i\zeta_2}{k})\kappa\cos\kappa(b-a)}\Phi_2^+(\alpha),\\&a\le y\le b,\end{aligned} \tag{45}$$

where the first term on the right hand side of (44) comes from the incident field.

Invoking (43) to (45) in (29) and (30), we arrive at

$$\begin{aligned}&\frac{-\kappa(\sin\kappa(b+a)+(\frac{\mathrm{i}\zeta_1}{k})\kappa\cos\kappa(b+a))\Phi_1^+(\alpha)}{\sin 2\kappa a(\sin\kappa(b-a)+(\frac{\mathrm{i}\zeta_1}{k})\kappa\cos\kappa(b-a))}\\&+\frac{\kappa\Phi_2^+(\alpha)}{\sin 2\kappa a}-\frac{\lambda_1}{\chi_1+\alpha}=\Phi_1^-(\alpha)\end{aligned} \tag{46}$$

and

$$\frac{\kappa(\sin\kappa(b+a)+(\frac{\mathrm{i}\zeta_2}{k})\kappa\cos\kappa(b+a))\Phi_2^+(\alpha)}{\sin 2\kappa a(\sin\kappa(b-a)+(\frac{\mathrm{i}\zeta_2}{k})\kappa\cos\kappa(b-a))} -\frac{\kappa\Phi_1^+(\alpha)}{\sin 2\kappa a}+\frac{\lambda_1}{\chi_1+\alpha}=\Phi_2^-(\alpha), \tag{47}$$

where

$$\lambda_1=\frac{-\mathrm{i}\pi}{2a}, \tag{48}$$

$$\Phi_1^-(\alpha)=\widehat{\Phi}'_-(\alpha,-a^-)-\widehat{\Phi}'_-(\alpha,-a^+), \tag{49}$$

and

$$\Phi_2^-(\alpha)=\widehat{\Phi}'_-(\alpha,a^-)-\widehat{\Phi}'_-(\alpha,a^+). \tag{50}$$

The functions $\Phi_1^-(\alpha)$ and $\Phi_2^-(\alpha)$ are analytic in the region $\operatorname{Im}\alpha<\operatorname{Im}k$. Solution of the above equations leads to the following:

$$-\frac{G_1(\alpha)\Phi_1^+(\alpha)}{W(\alpha)}+\frac{\Phi_2^+(\alpha)}{W(\alpha)}-\frac{\lambda_1}{\chi_1+\alpha}=\Phi_1^-(\alpha), \tag{51}$$

$$\frac{G_2(\alpha)\Phi_2^+(\alpha)}{W(\alpha)}-\frac{\Phi_1^+(\alpha)}{W(\alpha)}+\frac{\lambda_1}{\chi_1+\alpha}=\Phi_2^-(\alpha), \tag{52}$$

where

$$G_{1,2}(\alpha)=\frac{\sin\kappa(b+a)+(\frac{\mathrm{i}\zeta_{1,2}}{k})\kappa\cos\kappa(b+a)}{\sin\kappa(b-a)+(\frac{\mathrm{i}\zeta_{1,2}}{k})\kappa\cos\kappa(b-a)}, \tag{53}$$

and

$$W(\alpha)=\frac{\sin 2\kappa a}{\kappa}. \tag{54}$$

We note that (51) and (52) are two coupled equations which involve four unknowns $\Phi_1^\pm(\alpha)$, $\Phi_2^\pm(\alpha)$. These unknowns can be determined by the Wiener-Hopf procedure and the pole removal technique [15–18].

4. Solution of the Problem

Writing [see appendix]

$$G_{1,2}(\alpha)=G_{1,2}^+(\alpha)G_{1,2}^-(\alpha) \text{ and } W(\alpha)=W^+(\alpha)W^-(\alpha), \tag{55}$$

where the superscript (+) is assigned to the function regular in the upper half plane $\operatorname{Im}\alpha>-\operatorname{Im}k$ and superscript $(-)$ represents the function regular in the lower half plane $\operatorname{Im}\alpha<\operatorname{Im}k$. Now, from (51) and (52), we have

$$\frac{-G_1^+(\alpha)G_1^-(\alpha)\Phi_1^+(\alpha)}{W^+(\alpha)W^-(\alpha)}+\frac{\Phi_2^+(\alpha)}{W^+(\alpha)W^-(\alpha)} =\frac{\lambda_1}{\chi_1+\alpha}+\Phi_1^-(\alpha) \tag{56}$$

and

$$\frac{G_2^+(\alpha)G_2^-(\alpha)\Phi_2^+(\alpha)}{W^+(\alpha)W^-(\alpha)}-\frac{\Phi_1^+(\alpha)}{W^+(\alpha)W^-(\alpha)} =-\frac{\lambda_1}{\chi_1+\alpha}+\Phi_2^-(\alpha). \tag{57}$$

Multiplying (56) by $\frac{W^-(\alpha)}{G_1^-(\alpha)}$ and (57) by $\frac{W^-(\alpha)}{G_2^-(\alpha)}$, we obtain

$$\frac{-G_1^+(\alpha)\Phi_1^+(\alpha)}{W^+(\alpha)}+\frac{G_1^+(\alpha)\Phi_2^+(\alpha)}{W^+(\alpha)G_1(\alpha)} =\frac{\lambda_1 W^-(\alpha)}{(\chi_1+\alpha)G_1^-(\alpha)}+\frac{W^-(\alpha)\Phi_1^-(\alpha)}{G_1^-(\alpha)} \tag{58}$$

and

$$\frac{G_2^+(\alpha)\Phi_2^+(\alpha)}{W^+(\alpha)}-\frac{G_2^+(\alpha)\Phi_1^+(\alpha)}{W^+(\alpha)G_2(\alpha)} =-\frac{\lambda_1 W^-(\alpha)}{(\chi_1+\alpha)G_2^-(\alpha)}+\frac{W^-(\alpha)\Phi_2^-(\alpha)}{G_2^-(\alpha)}. \tag{59}$$

Applying the well-known Wiener-Hopf decomposition procedure [22] on (58) and (59), respectively, we arrive at

$$\frac{-G_1^+(\alpha)\Phi_1^+(\alpha)}{W^+(\alpha)}+\frac{G_1^+(\alpha)\Phi_2^+(\alpha)}{W^+(\alpha)G_1(\alpha)}-\frac{\lambda_1 W^+(\chi_1)}{(\chi_1+\alpha)G_1^+(\chi_1)} =\frac{\lambda_1}{(\chi_1+\alpha)}\left[\frac{W^-(\alpha)}{G_1^-(\alpha)}-\frac{W^+(\chi_1)}{G_1^+(\chi_1)}\right]+\frac{W^-(\alpha)\Phi_1^-(\alpha)}{G_1^-(\alpha)} \tag{60}$$

and

$$\frac{G_2^+(\alpha)\Phi_2^+(\alpha)}{W^+(\alpha)}-\frac{G_2^+(\alpha)\Phi_1^+(\alpha)}{W^+(\alpha)G_2(\alpha)}+\frac{\lambda_1 W^+(\chi_1)}{(\chi_1+\alpha)G_2^+(\chi_1)} =-\frac{\lambda_1}{(\chi_1+\alpha)}\left[\frac{W^-(\alpha)}{G_2^-(\alpha)}-\frac{W^+(\chi_1)}{G_2^+(\chi_1)}\right]+\frac{W^-(\alpha)\Phi_2^-(\alpha)}{G_2^-(\alpha)}. \tag{61}$$

In (60) and (61) the regularity of the left hand side in the upper half plane may be violated by the simple poles occurring at the zeros of $G_1(\alpha)$ and $G_2(\alpha)$ lying in the upper half plane, namely, at $\alpha = \mu_n$ and $\alpha = \nu_n$ ($n = 1,2,3,\ldots$), respectively [15]. By subtracting the infinite series of poles $\sum_{n=1}^{\infty} \frac{a_n}{\alpha-\mu_n}$ and $\sum_{n=1}^{\infty} \frac{b_n}{\alpha-\nu_n}$ from both sides of (60) and (61), respectively, we get

$$\begin{aligned}&\frac{-G_1^+(\alpha)\Phi_1^+(\alpha)}{W^+(\alpha)}+\frac{G_1^+(\alpha)\Phi_2^+(\alpha)}{W^+(\alpha)G_1(\alpha)}\\&-\frac{\lambda_1 W^+(\chi_1)}{(\chi_1+\alpha)G_1^+(\chi_1)}-\sum_{n=1}^{\infty}\frac{a_n}{\alpha-\mu_n}=\\&\quad\frac{\lambda_1}{(\chi_1+\alpha)}\left[\frac{W^-(\alpha)}{G_1^-(\alpha)}-\frac{W^+(\chi_1)}{G_1^+(\chi_1)}\right]\\&\quad+\frac{W^-(\alpha)\Phi_1^-(\alpha)}{G_1^-(\alpha)}-\sum_{n=1}^{\infty}\frac{a_n}{\alpha-\mu_n}\end{aligned}\tag{62}$$

and

$$\begin{aligned}&\frac{G_2^+(\alpha)\Phi_2^+(\alpha)}{W^+(\alpha)}-\frac{G_2^+(\alpha)\Phi_1^+(\alpha)}{W^+(\alpha)G_2(\alpha)}\\&+\frac{\lambda_1 W^+(\chi_1)}{(\chi_1+\alpha)G_2^+(\chi_1)}-\sum_{n=1}^{\infty}\frac{b_n}{\alpha-\nu_n}=\\&\quad-\frac{\lambda_1}{(\chi_1+\alpha)}\left[\frac{W^-(\alpha)}{G_2^-(\alpha)}-\frac{W^+(\chi_1)}{G_2^+(\chi_1)}\right]\\&\quad+\frac{W^-(\alpha)\Phi_2^-(\alpha)}{G_2^-(\alpha)}-\sum_{n=1}^{\infty}\frac{b_n}{\alpha-\nu_n}.\end{aligned}\tag{63}$$

The unwanted poles should satisfy following equations:

$$a_n=\frac{G_1^+(\mu_n)\Phi_2^+(\mu_n)}{W^+(\mu_n)G_1^*(\mu_n)},\quad n=1,2,3,\ldots,\tag{64}$$

and

$$b_n=-\frac{G_2^+(\nu_n)\Phi_1^+(\nu_n)}{W^+(\nu_n)G_2^*(\nu_n)},\quad n=1,2,3,\ldots,\tag{65}$$

where * denotes the differentiation with respect to α. Note that the left hand sides of (62) and (63) are analytic in $\operatorname{Im}\alpha > -\operatorname{Im}k$ and the right hand sides are analytic in $\operatorname{Im}\alpha < \operatorname{Im}k$. By the standard Wiener-Hopf procedure [22] (62) and (63) give, respectively,

$$\begin{aligned}&\frac{-G_1^+(\alpha)\Phi_1^+(\alpha)}{W^+(\alpha)}+\frac{G_1^+(\alpha)\Phi_2^+(\alpha)}{W^+(\alpha)G_1(\alpha)}\\&-\frac{\lambda_1 W^+(\chi_1)}{(\chi_1+\alpha)G_1^+(\chi_1)}-\sum_{n=1}^{\infty}\frac{a_n}{\alpha-\mu_n}=0\end{aligned}\tag{66}$$

and

$$\begin{aligned}&\frac{G_2^+(\alpha)\Phi_2^+(\alpha)}{W^+(\alpha)}-\frac{G_2^+(\alpha)\Phi_1^+(\alpha)}{W^+(\alpha)G_2(\alpha)}\\&+\frac{\lambda_1 W^+(\chi_1)}{(\chi_1+\alpha)G_2^+(\chi_1)}-\sum_{n=1}^{\infty}\frac{b_n}{\alpha-\nu_n}=0.\end{aligned}\tag{67}$$

The unknown constants a_n and b_n involved in the expressions of $\Phi_1^+(\alpha)$ and $\Phi_2^+(\alpha)$ can be evaluated through the system of $2\times N$ linear algebraic equations, where N stands for the approximately chosen upper limit related to the sum series of (66) and (67). By putting $\alpha=\mu_n$ and $\alpha=\nu_n$ for $n=1,2,3,\ldots$ we can have a linear system of algebraic equations

$$\begin{aligned}&\frac{G_2^+(\mu_n)G_1^*(\mu_n)}{G_1^+(\mu_n)}a_n-\sum_{n=1}^{\infty}\frac{b_n}{\mu_n-\nu_n}\\&+\frac{G_2^+(\mu_n)}{G_1^+(\mu_n)G_2(\mu_n)}\sum_{m=1}^{\infty}\frac{a_m\delta_{nm}}{\mu_n-\mu_m}=\\&-\frac{\lambda_1 W^+(\chi_1)}{(\chi_1+\mu_n)G_2^+(\chi_1)}\\&-\frac{\lambda_1 W^+(\chi_1)G_2^+(\mu_n)}{(\chi_1+\mu_n)G_2(\mu_n)G_1^+(\mu_n)G_1^+(\chi_1)},\end{aligned}\tag{68}$$

$$\begin{aligned}&\frac{G_1^+(\nu_n)G_2^*(\nu_n)}{G_2^+(\nu_n)}b_n-\sum_{n=1}^{\infty}\frac{a_n}{\nu_n-\mu_n}\\&+\frac{G_1^+(\nu_n)}{G_2^+(\nu_n)G_1(\nu_n)}\sum_{m=1}^{\infty}\frac{b_m\delta_{nm}}{\nu_n-\nu_m}=\\&\frac{\lambda_1 W^+(\chi_1)}{(\chi_1+\nu_n)G_1^+(\nu_n)}\\&+\frac{\lambda_1 W^+(\chi_1)G_1^+(\nu_n)}{(\chi_1+\nu_n)G_1(\nu_n)G_2^+(\nu_n)G_2^+(\chi_1)}.\end{aligned}\tag{69}$$

Here δ_{nm} is defined as

$$\delta_{nm}=\begin{cases}1, & n\neq m,\\ 0, & n=m.\end{cases}\tag{70}$$

Taking the inverse Fourier transform of (43) to (45), we obtain:

i) For the region ($-b\le y\le -a$, $x<0$), one may write

$$\begin{aligned}&\Phi(x,y)=\\&\frac{1}{2\pi}\int_{-\infty+\mathrm{i}\tau}^{\infty+\mathrm{i}\tau}\frac{\mathrm{e}^{-\mathrm{i}\alpha x}}{\sin\kappa(b-a)+\left(\frac{\mathrm{i}\zeta_1}{k}\right)\kappa\cos\kappa(b-a)}\Phi_1^+(\alpha)\\&\cdot\left\{\sin\kappa(y+b)+\left(\frac{\mathrm{i}\zeta_1}{k}\right)\kappa\cos\kappa(y+b)\right\}\mathrm{d}\alpha.\end{aligned}\tag{71}$$

ii) When $(-a \le y \le a, x < 0)$, we have

$$\Phi(x,y) = \mathrm{e}^{\mathrm{i}\chi_1 x} \sin\left[\frac{\pi(y-a)}{2a}\right] + \frac{1}{2\pi}\int_{-\infty+\mathrm{i}\tau}^{\infty+\mathrm{i}\tau} \frac{\mathrm{e}^{-\mathrm{i}\alpha x}}{\sin 2\kappa a} \cdot \left\{\Phi_2^+(\alpha)\sin\kappa(y+a) - \Phi_1^+(\alpha)\sin\kappa(y-a)\right\}\mathrm{d}\alpha. \quad (72)$$

iii) For $(a \le y \le b, x < 0)$, we arrive at

$$\Phi(x,y) = \frac{1}{2\pi}\int_{-\infty+\mathrm{i}\tau}^{\infty+\mathrm{i}\tau} \frac{\mathrm{e}^{-\mathrm{i}\alpha x}}{\sin\kappa(b-a) + \left(\frac{\mathrm{i}\zeta_2}{k}\right)\kappa\cos\kappa(b-a)} \Phi_2^+(\alpha) \cdot \left\{\sin\kappa(y-b) - \left(\frac{\mathrm{i}\zeta_2}{k}\right)\kappa\cos\kappa(y-b)\right\}\mathrm{d}\alpha. \quad (73)$$

In (71) to (73) τ is the imaginary part of α, $\kappa(\alpha) = \sqrt{k^2-\alpha^2}$, and branch cuts are taken to be from k to $\mathrm{i}\infty$ and $-k$ to $-\mathrm{i}\infty$, and $0 \le \arg\kappa \le \pi$ (Fig. 2).

Note that the integrands have no singularities which lie on the contour of integration. To evaluate the integrals in (71) to (73) it is noted that the contour of integration in these equations lies in the strip $-\mathrm{Im}k < \mathrm{Im}\alpha < \mathrm{Im}k$. The integrals can be evaluated by closing the contour in the upper half α-plane. Thus the only singularities in the integrands of (71) and (73) occur at the zeros of

$$\sin\kappa(b-a) + \left(\frac{\mathrm{i}\zeta_1}{k}\right)\kappa\cos\kappa(b-a) = 0,$$

which is at

$$\alpha = (k^2 - \widehat{\nu}_n^2)^{\frac{1}{2}} (n = 1,2,3,\ldots),$$

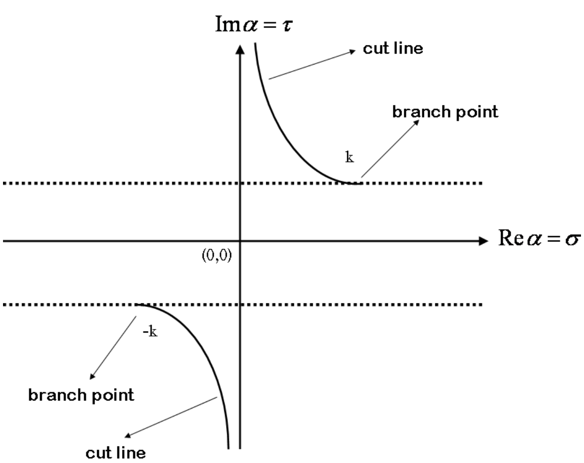

Fig. 2. Strip of analyticity and branch cuts in the complex α-plane.

and

$$\sin\kappa(b-a) + \left(\frac{\mathrm{i}\zeta_2}{k}\right)\kappa\cos\kappa(b-a) = 0,$$

which is at

$$\alpha = (k^2 - \widetilde{\nu}_n^2)^{\frac{1}{2}}, \quad n = 1,2,3,\ldots,$$

respectively. The only singularities in the integrands in (72) occur at the zeros of

$$\sin 2\kappa a = 0,$$

which is at

$$\alpha = (k^2 - \frac{n^2\pi^2}{4a^2})^{\frac{1}{2}}, \quad n = 1,2,3,\ldots.$$

5. Reflected Field Representation

Inside the waveguide field intensity is a superposition of a transmitted and a reflected wave. Thus it is relevant to deal with reflection/transmission coefficients which are related to 'relative energy'. The reflection coefficient of the first mode of the inside waveguide (which is the only propagative mode) is calculated from the contribution of the pole at $\alpha = \chi_1$ as

$$R = -\frac{\pi\mathrm{i}}{4a^2\chi_1}\left\{\Phi_1^+(\chi_1) + \Phi_2^+(\chi_1)\right\} \quad (74)$$

with

$$\Phi_1^+(\chi_1) + \Phi_2^+(\chi_1) = -\frac{\lambda_1(W^+(\chi_1))^2}{4\chi_1} \cdot \left\{\frac{1}{(G_1^+(\chi_1))^2} + \frac{1}{(G_2^+(\chi_1))^2}\right\} + \frac{W^+(\chi_1)}{2} \cdot \left\{\frac{1}{G_2^+(\chi_1)}\sum_{n=1}^{\infty}\frac{b_n}{\chi_1-\nu_n} - \frac{1}{G_1^+(\chi_1)}\sum_{n=1}^{\infty}\frac{a_n}{\chi_1-\mu_n}\right\}. \quad (75)$$

(75) is obtained by substituting $\alpha = \chi_1$ and $b = 2a$ in (66) and (67).

6. Numerical and Graphical Results

In this section some graphical results displaying the effects of physical and geometrical parameters on the propagation of sound in the trifurcated duct are presented. The ability of a surface to guide and support a surface wave can be determined by its surface

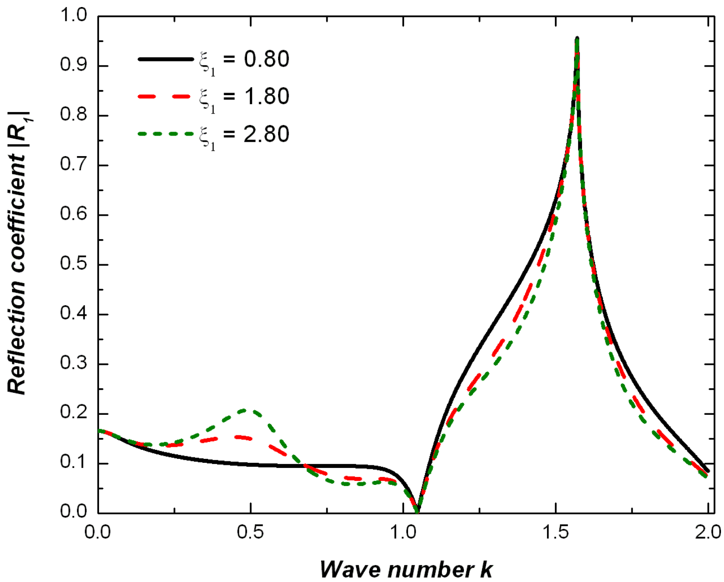

Fig. 3 (colour online). Plots showing profiles of $|R_1|$ versus k for different values of ζ_1 when $a = 1$, $b = 2a$, and $\zeta_2 = 0.30$.

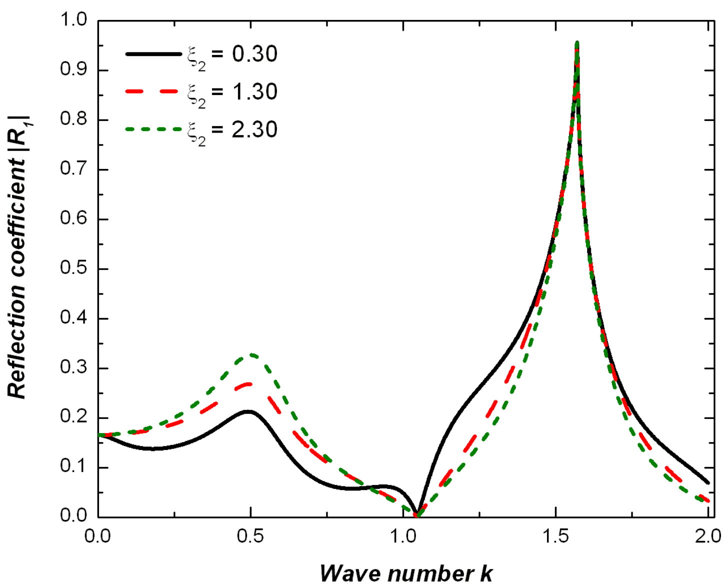

Fig. 4 (colour online). Plots showing profiles of $|R_1|$ versus k for different values of ζ_2 when $a = 1$, $b = 2a$, and $\zeta_1 = 2.90$.

impedance ζ, which is generally a complex number $\zeta = \xi + \mathrm{i}\eta$, where the real part ξ is the surface 'resistance' and the imaginary part η is the surface 'reactance'. The real part ξ is always non-negative. When real part $\xi = 0$, the surface is lossless and a surface wave can propagate on it without attenuation. When real part $\xi > 0$, the surface is lossy and the surface wave is attenuated. The imaginary part η can be positive or negative, then the surface is said to be 'capacitive' or 'inductive', respectively [23]. For wave bearing corrugated surfaces which do not absorb energy the complex specific impedance $\zeta = \xi - \mathrm{i}\eta$ has a zero resistive component $\xi = 0$, and a purely negative reactance $\eta < 0$ [24]. The values of the specific impedance $\zeta = \xi + \mathrm{i}\eta$ $(= z/\rho_0 c)$ for an absorbing sheet which seem to have practical importance are [12]:

Fibrous sheet: $\xi = 0.5, \quad -1 < \eta < 3,$
Perforated sheet: $0 < \xi < 3, \quad -1 < \eta < 3.$

We have used the Mathematica 5.2 software for the numerical evaluation and graphical representation of the functions given by (74).

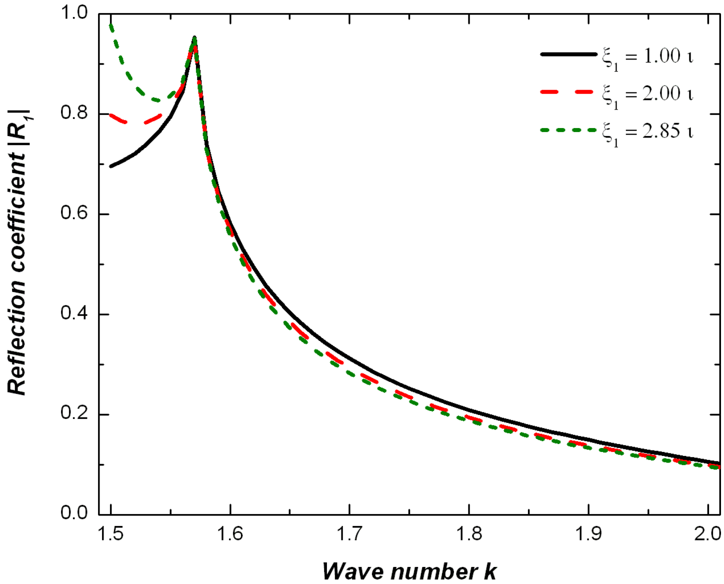

Fig. 5 (colour online). Plots showing profiles of $|R_1|$ versus k for different values of ζ_1 when $a = 1$, $b = 2a$, and $\zeta_2 = 0.001\mathrm{i}$.

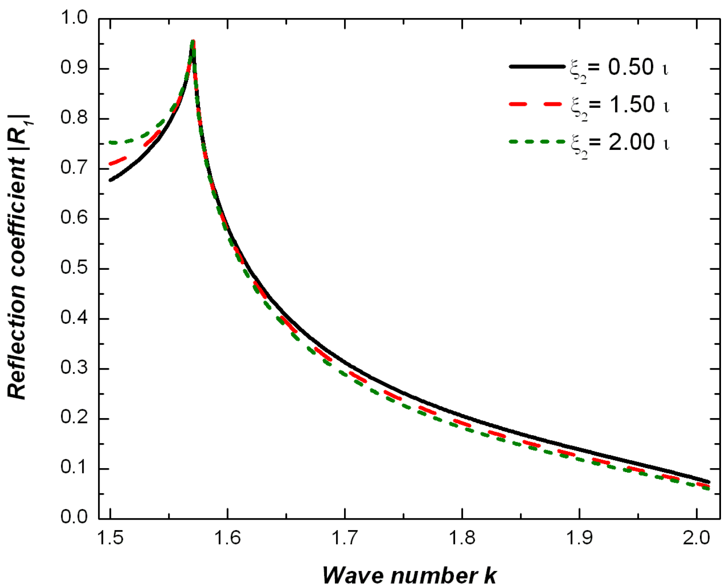

Fig. 6 (colour online). Plots showing profiles of $|R_1|$ versus k for different values of ζ_2 when $a = 1$, $b = 2a$, and $\zeta_1 = 0.30\mathrm{i}$.

Figures 3 and 4 depict the amplitude of the reflected field intensity against the wave number k for different values of noise reduction parameters, i. e. ξ_1 (keeping ζ_2 constant) and ξ_2 (ζ_1 is held fixed), respectively. The surface impedance taken is purely real, i. e; $\mathrm{Re}\,\xi_{1,2} > 0$ (resistance surface impedance). Figures 5 and 6 display the reflected field intensity in absolute form against the wave number k for different values of impedance parameters, i. e. ξ_1 (keeping ζ_2 constant) and ξ_2 (ζ_1 is held fixed), respectively. The surface impedance is taken purely imaginary, i.e. $\mathrm{Im}\,\xi_{1,2} > 0$ (capacitive surface impedance). Figures 7 and 8 show the plots of the reflected field intensity in absolute value against the wave number k for several values of noise reduction parameters, i. e. ξ_1 (keeping ζ_2 constant) and ξ_2 (ζ_1 is held fixed), respectively. Both real and imaginary parts of the surface impedance are taken into account.

In Figures 9 and 10 the reflected field intensity is plotted against the wave number k for various values of b (separation distance between the infinite plates).

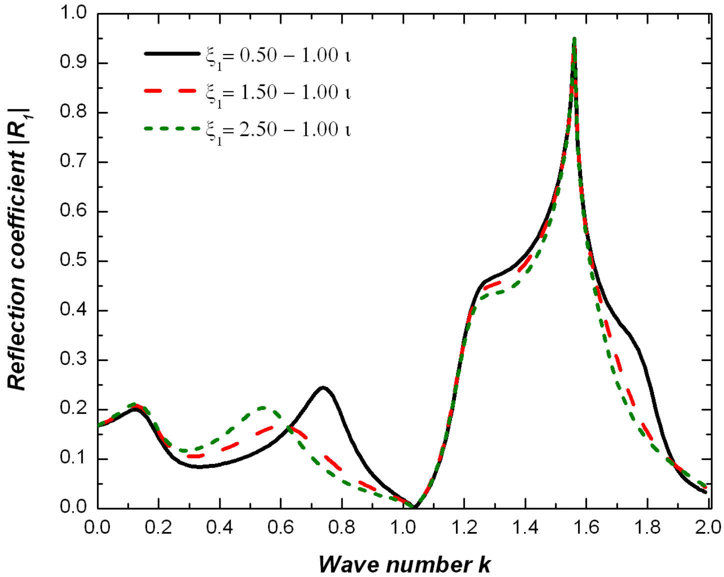

Fig. 7 (colour online). Plots showing profiles of $|R_1|$ versus k for different values of ζ_1 when $a=1$, $b=2a$, and $\zeta_2=0.30+0.50\text{i}$.

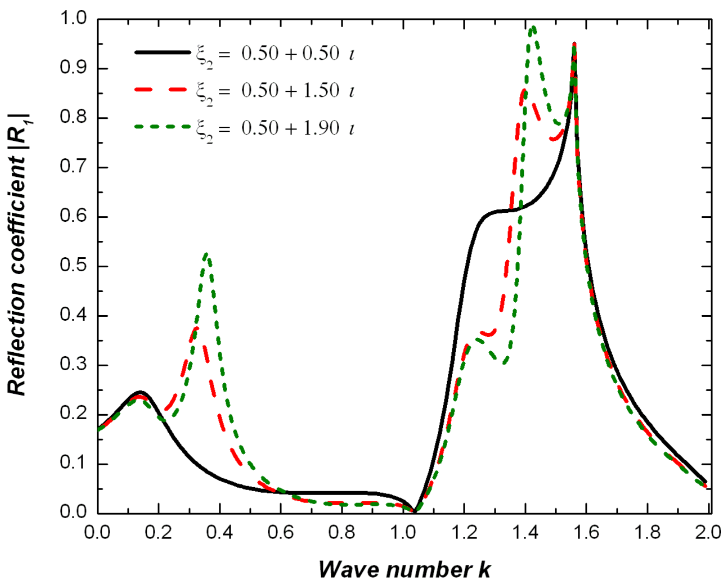

Fig. 8 (colour online). Plots showing profiles of $|R_1|$ versus k for different values of ζ_2 when $a=1$, $b=2a$, and $\zeta_1=0.30+0.50\text{i}$.

In Figure 9 the resistance surface impedance is considered only while in Figure 10 the surface impedance with both real and imaginary parts is analyzed. Figure 11 describes the amplitude of the reflected field intensity against the truncation number N for different values of wave number k. The surface impedance considered is imaginary, i. e. $\operatorname{Im}\xi_{1,2}>0$ (capacitive surface impedance).

The main findings are summarized in the following points:

- It is observed that the reflected field intensity of the first mode of the inside waveguide (which is the only propagative mode) decreases as we increase the values of the impedance parameters.
- As we gradually increase the separation distance b between the infinite plates, the value of the reflected field intensity $|R_1|$ decreases.
- The reflected field intensity becomes insensitive to the truncation number $N>4$. We require a small N for a decreasing value of k since the total field also decreases. By taking into account this criterion, N can be chosen for numerical examples.

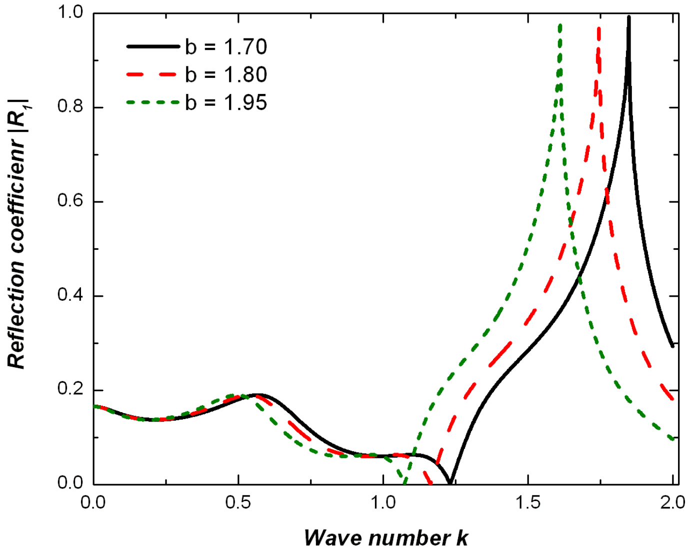

Fig. 9 (colour online). Plots showing profiles of $|R_1|$ versus k for different values of b when $a = b/2$, $\zeta_1 = 0.30$, and $\zeta_2 = 2.50$.

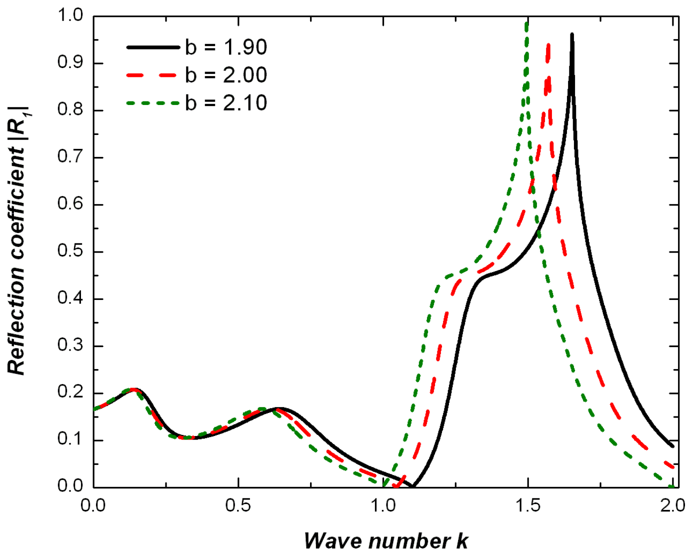

Fig. 10 (colour online). Plots showing profiles of $|R_1|$ versus k for different values of b when $a = b/2$, $\zeta_1 = 1.50 - 1.00\mathrm{i}$, and $\zeta_2 = 0.30 + 0.50\mathrm{i}$.

- It is worth noticing from the mathematical analysis that for $b = 2a$ ($3a$ or $5a$), the parameters involved in the analysis show good attenuation results.
- The absolute values of the reflection coefficient $|R_1|$ obey the rules of conservation of energy.
- The radiated power from the semi-infinite guide which spreads among the different regions of the duct for the first mode, is proportional to $(1 - |R_1|^2)$ [1].

7. Final Remarks

The analysis of the trifurcated parallel plate waveguide with two semi-infinite acoustically soft plates placed symmetrically inside two infinite acoustically lined plates is accomplished rigorously by means of the Wiener-Hopf technique. The surface impedances of the upper and the lower infinite plates are different from each other. A sound wave of first mode propagating out of the mouth of the semi-infinite soft duct is taken into account. Because of the generality and asymmetry of the boundary conditions, an approximate solution is evaluated rather than having a closed form solution. First, we reduce the problem into two coupled modified Wiener-Hopf equations and then solve it by using Wiener-Hopf procedure and pole removal technique. Two sets of infinitely many unknown coefficients sat-

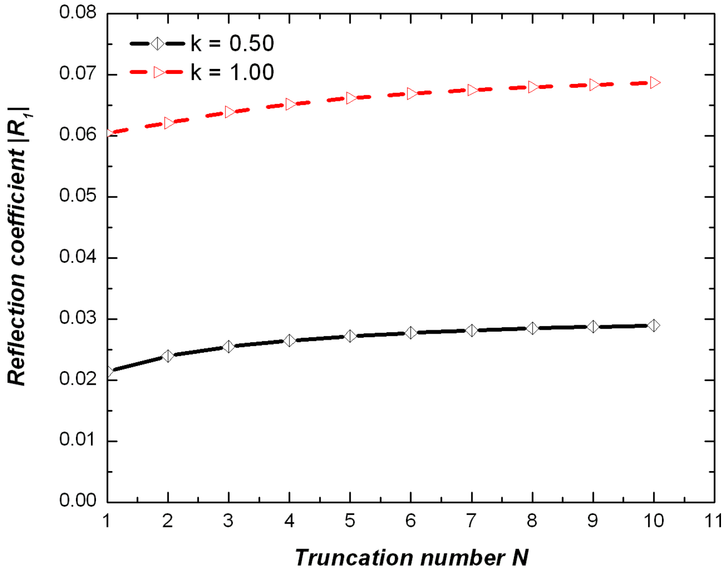

Fig. 11 (colour online). Plots showing profiles of $|R_1|$ versus truncation number N when $b = 2a$, $a = 1$, $\zeta_1 = 0.50\mathrm{i}$, and $\zeta_2 = 0.10\mathrm{i}$.

isfying two infinite systems of linear algebraic equations are involved in the solution. These unknown coefficients are evaluated numerically. We observe that the reflected field amplitude being calculated does not change to a given number of decimal places for a given set of the problem parameters. This reveals that the expansions are numerically convergent. Some graphs are plotted for sundry parameters using the reflection coefficient of first mode in absolute value versus wave number. It is observed that soft and impedance surfaces show good noise reduction effects on the noise transmitted through the waveguide. The results have possible applications to duct acoustics and noise reduction devices. This investigation contains different combinations of boundary conditions. The results for limiting cases can be obtained from this analysis.

Acknowledgement

The authors greatly appreciate the anonymous reviewers for valuable suggestions to improve the quality of the paper.

Appendix

Now, we come to the mathematical maneuver that is central to the Wiener-Hopf equation. We factorize kernel functions. The factorization of the kernel functions $G_{1,2}(\alpha)$ and $W(\alpha)$ is of the form

$$G_{1,2}(\alpha) = G^+_{1,2}(\alpha)G^-_{1,2}(\alpha) \text{ and}$$
$$W(\alpha) = W^+(\alpha)W^-(\alpha),$$

where $G^+_{1,2}(\alpha)$ and $W^+(\alpha)$ denote certain functions which are regular and free of zeros in the upper half plane $\operatorname{Im}\alpha > -\operatorname{Im}k$, and $G^-_{1,2}(\alpha)$ and $W^-(\alpha)$ denote certain functions which are regular and free of zeros in the lower half plane $\operatorname{Im}\alpha < \operatorname{Im}k$.

We may note that the functions $G_{1,2}(\alpha)$ and $W(\alpha)$ are even in the Fourier transform parameter α and, more precisely, their respective derivatives are zero at $\alpha = 0$. So these functions can be factorized by applying the infinite product expansion of an integral function with infinitely many zeros [22, 25]. For given $G_{1,2}(\alpha)$ by (53) we have

$$G_{1,2}(\alpha) = \frac{\sin\kappa(b+a) + (\frac{\mathrm{i}\zeta_{1,2}}{k})\kappa\cos\kappa(b+a)}{\sin\kappa(b-a) + (\frac{\mathrm{i}\zeta_{1,2}}{k})\kappa\cos\kappa(b-a)}$$

or

$$G_{1,2}(\alpha) = \frac{L_{1,3}(\alpha)}{L_{2,4}(\alpha)}.$$

By employing the procedure outlined by Mittra and Lee [26], we have

$$L^+_1(\alpha) = \sqrt{\sin k(b+a) + \mathrm{i}\zeta_1\cos k(b+a)}$$
$$\cdot \exp\left\{\frac{\mathrm{i}\alpha(b+a)}{\pi}\left[1 - C - \ln\left(\frac{|\alpha|(b+a)}{\pi}\right) + \frac{\mathrm{i}\pi}{2}\right]\right\}$$
$$\cdot \prod_{n=1}^{\infty}\left(1 + \frac{\alpha}{\mu_n}\right)\exp\left(\frac{\mathrm{i}\alpha(b+a)}{n\pi}\right),$$

$$L_2^+(\alpha) = \sqrt{\sin k(b-a) + \mathrm{i}\zeta_1 \cos k(b-a)}$$
$$\cdot \exp\left\{\frac{\mathrm{i}\alpha(b-a)}{\pi}\left[1 - C - \ln\left(\frac{|\alpha|(b-a)}{\pi}\right) + \frac{\mathrm{i}\pi}{2}\right]\right\}$$
$$\cdot \prod_{n=1}^{\infty}\left(1 + \frac{\alpha}{\widehat{\nu}_n}\right)\exp\left(\frac{\mathrm{i}\alpha(b-a)}{n\pi}\right),$$
$$L_3^+(\alpha) = \sqrt{\sin k(b+a) + \mathrm{i}\zeta_2 \cos k(b+a)}$$
$$\cdot \exp\left\{\frac{\mathrm{i}\alpha(b+a)}{\pi}\left[1 - C - \ln\left(\frac{|\alpha|(b+a)}{\pi}\right) + \frac{\mathrm{i}\pi}{2}\right]\right\}$$
$$\cdot \prod_{n=1}^{\infty}\left(1 + \frac{\alpha}{\widetilde{\mu}_n}\right)\exp\left(\frac{\mathrm{i}\alpha(b+a)}{n\pi}\right),$$

and

$$L_4^+(\alpha) = \sqrt{\sin k(b-a) + \mathrm{i}\zeta_2 \cos k(b-a)}$$
$$\cdot \exp\left\{\frac{\mathrm{i}\alpha(b-a)}{\pi}\left[1 - C - \ln\left(\frac{|\alpha|(b-a)}{\pi}\right) + \frac{\mathrm{i}\pi}{2}\right]\right\}$$
$$\cdot \prod_{n=1}^{\infty}\left(1 + \frac{\alpha}{\widetilde{\nu}_n}\right)\exp\left(\frac{\mathrm{i}\alpha(b-a)}{n\pi}\right)$$

with

$$G_{1,2}^+(\alpha) = \frac{L_{1,3}^+(\alpha)}{L_{2,4}^+(\alpha)}.$$

Thus,

$$G_{1,2}(\alpha) = G_{1,2}^+(\alpha)G_{1,2}^-(\alpha),$$

where

$$G_1^+(\alpha) = \sqrt{\frac{\sin k(b+a) + \mathrm{i}\zeta_1 \cos k(b+a)}{\sin k(b-a) + \mathrm{i}\zeta_1 \cos k(b-a)}}$$
$$\cdot \frac{\exp\left\{\frac{\mathrm{i}\alpha(b+a)}{\pi}\left[1 - C - \ln\left(\frac{|\alpha|(b+a)}{\pi}\right) + \frac{\mathrm{i}\pi}{2}\right]\right\}}{\exp\left\{\frac{\mathrm{i}\alpha(b-a)}{\pi}\left[1 - C - \ln\left(\frac{|\alpha|(b-a)}{\pi}\right) + \frac{\mathrm{i}\pi}{2}\right]\right\}}$$
$$\cdot \prod_{n=1}^{\infty}\frac{(1 + \frac{\alpha}{\mu_n})\exp\left(\frac{\mathrm{i}\alpha(b+a)}{n\pi}\right)}{(1 + \frac{\alpha}{\widehat{\nu}_n})\exp\left(\frac{\mathrm{i}\alpha(b-a)}{n\pi}\right)}$$

and

$$G_2^+(\alpha) = \sqrt{\frac{\sin k(b+a) + \mathrm{i}\zeta_2 \cos k(b+a)}{\sin k(b-a) + \mathrm{i}\zeta_2 \cos k(b-a)}}$$
$$\cdot \frac{\exp\left\{\frac{\mathrm{i}\alpha(b+a)}{\pi}\left[1 - C - \ln\left(\frac{|\alpha|(b+a)}{\pi}\right) + \frac{\mathrm{i}\pi}{2}\right]\right\}}{\exp\left\{\frac{\mathrm{i}\alpha(b-a)}{\pi}\left[1 - C - \ln\left(\frac{|\alpha|(b-a)}{\pi}\right) + \frac{\mathrm{i}\pi}{2}\right]\right\}}$$
$$\cdot \prod_{n=1}^{\infty}\frac{(1 + \frac{\alpha}{\widetilde{\mu}_n})\exp\left(\frac{\mathrm{i}\alpha(b+a)}{n\pi}\right)}{(1 + \frac{\alpha}{\widetilde{\nu}_n})\exp\left(\frac{\mathrm{i}\alpha(b-a)}{n\pi}\right)}.$$

Here, μ_n's, $\widehat{\nu}_n$'s, $\widetilde{\mu}_n$'s, and $\widetilde{\nu}_n$'s are the roots of the functions $L_1(\alpha)$, $L_2(\alpha)$, $L_3(\alpha)$, and $L_4(\alpha)$, respectively:

$$L_1(\mu_n) = 0, \quad L_2(\widehat{\nu}_n) = 0, \quad L_3(\widetilde{\mu}_n) = 0,$$
$$\text{and } L_4(\widetilde{\nu}_n) = 0, \quad n = 1, 2, 3, \ldots$$

with

$$L_1^-(\alpha) = L_1^+(-\alpha), \quad L_2^-(\alpha) = L_2^+(-\alpha),$$
$$L_3^-(\alpha) = L_3^+(-\alpha), \text{ and } L_4^-(\alpha) = L_4^+(-\alpha),$$

C being the Euler constant given by $C = 0.57721\ldots$ and $G_{1,2}^-(\alpha) = G_{1,2}^+(-\alpha)$. In the respective region of analyticity when $|\alpha| \to \infty$ then

$$G_{1,2}^{\pm}(\alpha) = O(1).$$

Similarly for $W(\alpha)$, given by (54), we have

$$W^{\pm}(\alpha) = \sqrt{\frac{\sin 2ka}{k}}$$
$$\cdot \exp\left\{\frac{2\mathrm{i}\alpha a}{\pi}\left[1 - C - \ln\left(\frac{2a|\alpha|}{\pi}\right) + \frac{\mathrm{i}\pi}{2}\right]\right\}$$
$$\cdot \prod_{n=1}^{\infty}\left(1 + \frac{\alpha}{\widehat{\sigma}_n}\right)\exp\left(\frac{2\mathrm{i}\alpha a}{n\pi}\right),$$

where $\widehat{\sigma}_n$ are the roots of the functions $W(\alpha)$:

$$W(\widehat{\sigma}_n) = 0, \quad n = 1, 2, 3, \ldots$$

with

$$W^-(\alpha) = W^+(-\alpha).$$

Also, when $|\alpha| \to \infty$ then in the respective region of analyticity

$$W^{\pm}(\alpha) = O(|\alpha|^{-\frac{1}{2}}).$$

[1] M. Hassan and A. D. Rawlins, Can. J. Physics **1**, 375 (1997).
[2] A. D. Rawlins, Math. Proc. Camb. Phil. Soc. **121**, 555 (1997).
[3] M. Hassan and A. D. Rawlins, Wave Motion **29**, 157 (1999).
[4] A. Snakowska, Eur. Phy. J. Special Topics **154**, 201 (2008).
[5] M. Ayub, M. H. Tiwana, and A. B. Mann, Commun. Nonlinear Sci. Numer. Simul. **14**, 3578 (2009).
[6] A. Büyükaksoy and B. Polat, ARI **51**, 196 (1999).
[7] B. Polat, Can. J. Phys. **76**, 771 (1998).
[8] A. Büyükaksoy and B. Polat, IEEE Trans. Antennas Propagat. **46**, 1692 (1998).
[9] D. S. Jones, Proc. R. Soc. London A **404**, 299 (1986).
[10] S. Asghar, M. Ayub, and B. Ahmad, Wave Motion **15**, 201 (1992).
[11] S. Asghar and T. Hayat, Acoustic Lett. **20** (9), 185 (1997).
[12] A. D. Rawlins and M. Hassan, Z. Angew. Math. Mech. **8**(5), 333 (2003).
[13] M. Ayub, M. H. Tiwana, and A. B. Mann, Physica Scripta **81**, 035402 (2010).
[14] I. D. Abrahams, Wave Motion **9**, 289 (1987).
[15] A. Büyükaksoy, I. H. Tayyar, and G. Uzgören, Influence of the junction of perfectly conducting and impedance parallel plate semi-infinite waveguides to the dominant mode propagation, First European Conference on Antennas and Propagation, Eu CAP Nice France 2006.
[16] M. Ayub, M. H. Tiwana, and A. B. Mann, Commun. Nonlinear Sci. Numer. Simul. **15**, 3939 (2010).
[17] I. H. Tayyar, A. Büyükaksoy, and A. Isikyer, Can. J. Physics **86**, 733 (2008).
[18] I. H. Tayyar, A. Büyükaksoy, and A. Isikyer, Radio Science **43**, RS5005, doi:10.1029/2007RS003768 (2008).
[19] A. D. Rawlins, Proc. R. Soc. London A **361**, 65 (1978).
[20] P. M. Morse and K. Ingard, Linear Acoustic Theory in: Handbuck der Akustik I, edited by S. Flügge, Springer, Berlin 1961, pp. 1 – 128.
[21] D. S. Jones, The Theory of Electromagnetism, Pergamon Press, London 1964.
[22] B. Noble, Methods Based on the Wiener-Hopf Technique, 2nd edn. Chelsea Publishing Company, New York 1988.
[23] J. Lam, J. Appl. Phys. **66** (8), 3437 (1989).
[24] A. D. Rawlins, J. Eng. Math **59**, 419 (2007).
[25] E. C. Titchmarsh, Theory of Fourier Integrals, University Press, Oxford 1937.
[26] R. Mittra and S. W. Lee, Analytical Techniques in the Theory of Guided Waves, McMillan, New York 1971.